

## Breakdown of a Topological Phase: Quantum Phase Transition in a Loop Gas Model with Tension

Simon Trebst,<sup>1</sup> Philipp Werner,<sup>2</sup> Matthias Troyer,<sup>3</sup> Kirill Shtengel,<sup>4</sup> and Chetan Nayak<sup>1,5</sup>

<sup>1</sup>Microsoft Research, Station Q, University of California, Santa Barbara, California 93106, USA

<sup>2</sup>Department of Physics, Columbia University, 538 West 120th Street, New York, New York 10027, USA

<sup>3</sup>Theoretische Physik, Eidgenössische Technische Hochschule Zürich, CH-8093 Zürich, Switzerland

<sup>4</sup>Department of Physics and Astronomy, University of California, Riverside, California 92521, USA

<sup>5</sup>Department of Physics and Astronomy, University of California, Los Angeles, California 90095, USA

(Received 6 September 2006; published 13 February 2007)

We study the stability of topological order against local perturbations by considering the effect of a magnetic field on a spin model—the toric code—which is in a topological phase. The model can be mapped onto a quantum loop gas where the perturbation introduces a bare loop tension. When the loop tension is small, the topological order survives. When it is large, it drives a continuous quantum phase transition into a magnetic state. The transition can be understood as the condensation of “magnetic” vortices, leading to confinement of the elementary “charge” excitations. We also show how the topological order breaks down when the system is coupled to an Ohmic heat bath and relate our results to error rates for topological quantum computations.

DOI: [10.1103/PhysRevLett.98.070602](https://doi.org/10.1103/PhysRevLett.98.070602)

PACS numbers: 05.50.+q, 03.65.Vf, 03.67.Lx, 75.10.-b

Topological phases are among the most remarkable phenomena in nature. Although the underlying interactions between electrons in a solid are not topologically invariant, their low-energy properties are. This enhanced symmetry makes such phases an attractive platform for quantum computation since it isolates the low-energy degrees of freedom from local perturbations—a usual cause of errors [1]. Tractable theoretical models with topological phases in frustrated magnets [1,2], Josephson junction arrays [3,4], or cold atoms in traps [5] have been proposed. However, such phases have not, thus far, been seen experimentally outside of the quantum Hall regime. Is this because topological phases are very rare and these models are adiabatically connected only to very small regions of the phase diagrams of real experimental systems?

In this Letter, we take a first step toward answering this question. We begin with the simplest exactly soluble model of a topological phase [1], whose Hamiltonian given below describes a frustrated magnet with four-spin interactions similar to cyclic ring exchanges. It is closely related to, and has the same topological phase as the quantum dimer model [6,7], which can be realized in Josephson junction arrays [3]. We consider perturbations of the soluble model that, when sufficiently large, drive the system out of the topological phase. The question is, how large? A small answer would imply that such a topological phase is delicate and occupies a small portion of the phase diagram. This might explain the paucity of experimentally observed topological phases. Instead, we find that “sufficiently large” is of order one in units of the basic four-spin plaquette interaction. Our numerical simulations demonstrate key signatures of the phase transition out of the topological phase, including the finite-size degeneracy splitting of the topological sectors, the condensation of magnetic excitations, and the confinement of electric charges.

We also consider perturbing the system by coupling it to an Ohmic heat bath. When coupled to such a bath, a quantum mechanical degree of freedom can undergo a transition from coherent to incoherent behavior [8]. Recently, the effects of such a coupling on quantum phase transitions, at which divergent numbers of quantum mechanical degrees of freedom interact, have been studied [9]. In both contexts, the coupling to the heat bath tends to make the system more classical. Coherent quantum oscillations are suppressed, while broken symmetry phases—which are essentially classical—are stabilized. A topological phase is quantum mechanical in nature. We find that coupling the heat bath to the kinetic energy does not destroy such a phase. However, for strong dissipation the gap becomes very small, and the topological phase may be too delicate to observe or use at reasonable temperatures. If the heat bath is coupled to the classical state of each plaquette, the topological phase is destroyed through a Kosterlitz-Thouless transition at a dissipation strength of order one.

In quantum information language the ground states in different topological sectors are the basis states of an encoded quantum memory. Quasiparticle excitations are states outside of the code subspace. The stability of the topological phase, as measured by a gap  $\Delta$  within a topological sector, translates into an error rate for topological qubits. At zero temperature, errors are due to the virtual excitation of pairs of quasiparticles, assuming that the system is shielded from perturbations at frequencies higher than  $\Delta$ . Such virtual processes lead to a splitting between topological sectors  $\delta E \sim e^{-\Delta L/v}$ , where  $L$  is the system size and  $v$  is a characteristic velocity. With increasing temperature, the thermal excitation of particles eventually dominates and the error rate is  $\sim e^{-\beta\Delta}$  [10].

*The model.*—We start with the toric code Hamiltonian

$$H_{\text{TC}} = -A \sum_v \prod_{j \in \text{vertex}(v)} \sigma_j^z - B \sum_p \prod_{j \in \text{plaquette}(p)} \sigma_j^x, \quad (1)$$

where the  $\sigma_i$  are  $S = 1/2$  quantum spins on  $2N$  edges of a square lattice with  $N$  vertices on a torus. Since all terms in (1) commute with each other, the model can be solved exactly [1]. The ground-state manifold can be described as a quantum loop gas where loops consist of chains of up-pointing  $\sigma^z$ -spins and the loop fugacity is  $d = 1$ . On the torus there are four degenerate ground states that can be classified by a winding number parity  $P_{y/x} = \prod_{i \in c_{x/y}} \sigma_i^z$  along a cut  $c_{x/y}$  in the  $x$  or  $y$  direction.

Here we study the effect of perturbing Hamiltonian (1) with a loop tension introduced either by a longitudinal magnetic field or local Ising interaction of the form

$$H = H_{\text{TC}} - h \sum_i \sigma_i^z - J \sum_{\langle ij \rangle} \sigma_i^z \sigma_j^z, \quad (2)$$

where  $h$  ( $J$ ) is the strength of the magnetic field (Ising interaction). These are the dominant perturbations expected in a physical implementation; e.g., in a Josephson junction implementation [3,4] they arise from electric potential perturbations or Coulomb interactions between neighboring quantum dots. We discuss this model in the limit of a large charge gap, i.e.,  $A \gg B$ ,  $h$ ,  $J$ , where it becomes equivalent to the “even” Ising gauge theory, the emergent gauge theory description of the quantum dimer model [13]. The low-energy sector has no free charges and any state is described by a collection of loops that can be obtained from a reference state (e.g., all  $\sigma_i^z = 1/2$ ) by a sequence of plaquette flips. Let us introduce a new plaquette spin operator  $\mu_p$  with eigenvalues  $\mu_p^z = (-1)^{n_p}/2$ , where  $n_p$  is the number of times a given plaquette  $p$  has been flipped, counting from the reference state. Then  $\sigma_i^z = 2\mu_p^z \mu_q^z$ , where  $p$  and  $q$  are the plaquettes separated by the edge  $i$ . The plaquette flip term in Eq. (1) becomes  $-4B \sum_p \mu_p^x$ . In the new variables, Hamiltonian (2) becomes equivalent to the transverse field Ising model (with both nearest and next-nearest-neighbor Ising interactions resulting from, respectively, the magnetic field  $h$  and the local Ising interaction  $J$  in the original Hamiltonian) in a basis restricted to loop states. With only the nearest-neighbor interaction (i.e.,  $J = 0$ ), this system orders at a critical field strength  $(h/B)_c = 0.65695(2)$  determined by continuous-time quantum Monte Carlo simulations [14]. Including the next-nearest-neighbor couplings ( $J \neq 0$ ) will lower the critical value somewhat without changing the nature of the transition, so we will concentrate on the  $J = 0$  case henceforth. The transverse field Ising model for the plaquette spins can be mapped to a classical  $(2 + 1)$ -dimensional Ising model:

$$\mathcal{H}_{\text{cl}} = -K_\tau \sum_{k,p} S_k^p S_{k+1}^p - K \sum_{k,\langle p,q \rangle} S_k^p S_k^q, \quad (3)$$

where  $S_k^p = S^p(k\Delta\tau)$  and  $S^p \equiv 2\mu_p^z = \pm 1$ . The real-space coupling is then given by  $K = \frac{1}{2}\Delta\tau h$  and the imaginary-time one by  $K_\tau = -\frac{1}{2}\ln[\tanh(\Delta\tau B)]$ , with  $\Delta\tau$  being the lattice spacing in the imaginary-time direction. The model (3) describes the well-known continuous mag-

netic phase transition of the 3D Ising model [15]. For isotropic interactions,  $K = K_\tau$ , the critical coupling has been determined with high precision to be  $K_c = 0.221\,659\,5(26)$  [17]. Setting  $B = 1$  this gives a critical loop tension  $h_c = 0.582\,24$  with  $\Delta\tau \approx 0.76$ . This value slightly varies from that for continuous time, but both models have the same long-distance physics. In Fig. 2, we use continuous time, in the other figures, discrete time.

The magnetic susceptibility diverges at the transition and the magnetization  $\langle \sum_i \sigma_i^z \rangle / 2N$  has a corresponding kink, shown in Fig. 1. This is not a symmetry-breaking transition, but the analogous transition driven by next-nearest interaction  $J$  is a *continuous* quantum phase transition from a topologically ordered quantum state to a broken symmetry state [18]. The transition can be understood in terms of the condensation of “magnetic vortices”, plaquettes with  $\prod_j \sigma_j^z = -1$ . The gap, which is  $\Delta = 2B$  for Hamiltonian (1), vanishes at  $h_c$ , as shown in Fig. 2. The gap has been estimated from measurements of the imaginary-time correlation length  $\xi_\tau$  as  $\Delta \propto 1/\xi_\tau$ , which we have calculated applying continuous-time quantum Monte Carlo simulations using the ALPS looper code [19,20].

*Topological order.*—The breakdown of topological order at the phase transition can be seen from the energy splitting  $\delta E$  between the ground states for the various sectors. When winding parities are used as basis states for a quantum memory, this splitting causes phase errors. (The absence of “electric charges” precludes any transitions between different winding parities so bit flip errors cannot occur.) In the topological phase, the virtual excitation of quasiparticles leads to a small splitting  $\delta E \propto \exp(-\Delta L/v)$  between the topological sectors. In the classically ordered phase, on the other hand, the energy splitting should scale with  $L$ , which corresponds to the energy cost of a loop in the ordered ground state. As the winding parity is conserved by imaginary-time spin-flip operations, we can simulate the system in one of the topological sectors by choosing an appropriate initial spin configura-

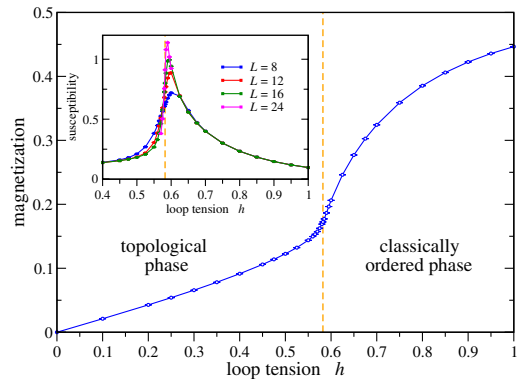


FIG. 1 (color online). Magnetization  $M$  versus loop tension. For small tension an almost constant susceptibility (see inset) leads to a linear increase of  $M$ . Above the critical loop tension (dashed line) the system approaches the fully polarized state.

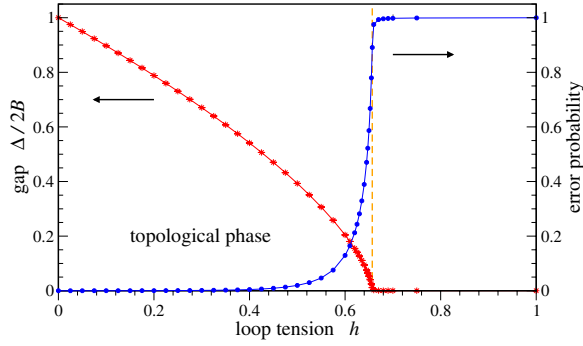


FIG. 2 (color online). Excitation gap for magnetic vortices (star symbols) versus loop tension. Right: Tunneling rate  $\exp(-\beta\Delta)$  between topological sectors (circles) for  $\beta = 10$ .

tion. Figure 3 shows the splitting for various system sizes in the vicinity of  $h_c$ . At the phase transition, the behavior changes from power-law scaling for strong loop tension to an exponential suppression in the topological phase for small loop tension. A more quantitative picture arises from the finite-size scaling analysis of the energy splitting  $\delta E(L)$  between the {even-odd}- and {even-even}-parity sectors shown in Fig. 4. For the critical loop tension we find a power-law scaling  $\delta E(L) \propto L^{2-z}$  with an exponent  $z = 1.42 \pm 0.02$ . Below the critical value the scaling turns into exponential scaling as expected for the topological phase.

**Confinement transition.**—For the loop gas (1) the elementary electric charge excitations (end points of an open loop) are deconfined. For strong loop tension, however these excitations are expected to become confined, thereby eliminating all open loops. In our simulations this transition is studied by breaking a loop in an arbitrary closed loop configuration and sampling the movement of the two end points. This allows us to measure the confinement length  $\xi_c$  as the square root of the average second moment of the distance between the two excitations, which for a torus with even extent  $L$  is normalized by a factor  $6/(L^2 + 2)$ . As shown in Fig. 5, electric charges clearly remain deconfined for the full extent of the topological phase

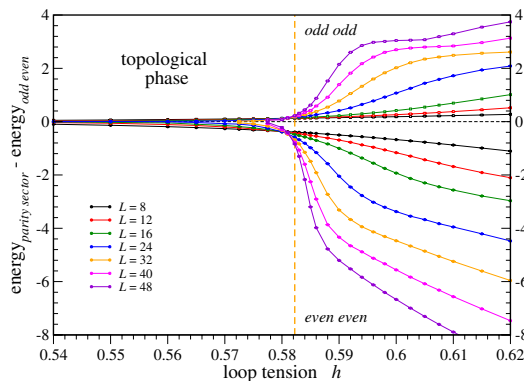


FIG. 3 (color online). Energy splitting between topological sectors. The sector with {even-odd/odd-even} winding number parities was taken as a reference (dashed line).

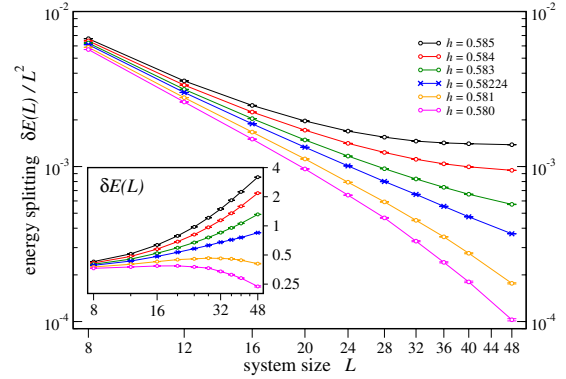


FIG. 4 (color online). Finite-size scaling of the energy splitting between topological sectors around the phase transition for  $\beta = 10L$ . At the critical loop tension (crosses) we find power-law scaling with exponent  $z = 1.42 \pm 0.02$ .

and the confinement transitions occurs simultaneously with the magnetic transition. At the critical loop tension the confinement lengths  $\xi_c(L)$  for various system sizes cross which demonstrates that the confinement length diverges with the *same* critical exponents as the magnetic correlation length  $\xi$  and there is only one length scale describing the phase transition. For our model without dynamical electric charges, this measure of the confinement of test charges is closely related to the calculation of a Wilson loop expectation value. In the presence of dynamical electric charges, Polyakov loops have been used as order parameter for the *finite* temperature transition of the 3D Ising gauge model [21].

**Dissipation.**—Finally, we discuss the effect of dissipation when Hamiltonian (1) is coupled to an Ohmic heat bath. We first examine coupling a heat bath to the kinetic energy, e.g., to  $\mu_p^x$ , so that a “phonon” is created when a plaquette flips. This type of dissipation could occur in a Josephson junction model [22] or in a spin model through the spin-phonon coupling. The standard procedure [23] for a linear spectral density (“Ohmic” dissipation) results in an effective action for independent Ising chains with long-

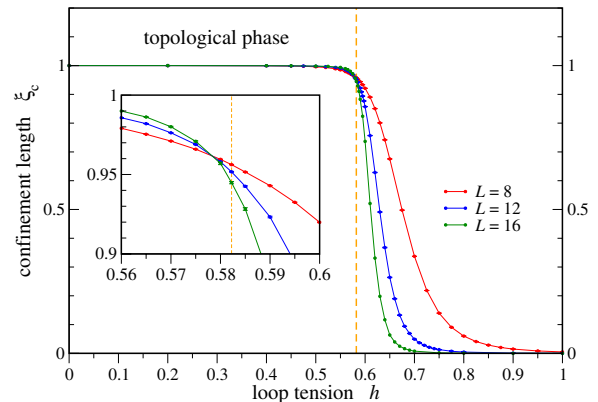


FIG. 5 (color online). Confinement length of electric charge excitations. The confinement transition occurs at the same critical loop tension (dashed line) as the magnetic transition.

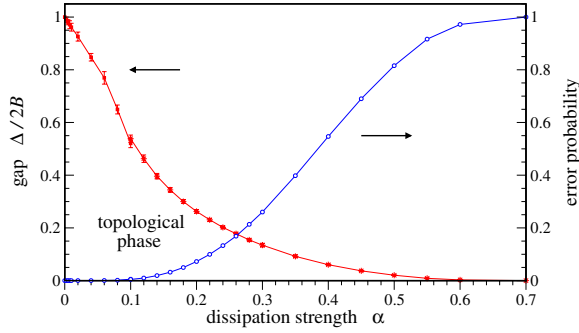


FIG. 6 (color online). Gap and error probability versus dissipation strength of the dissipative Ising chain (4).

range couplings in an external *longitudinal* magnetic field. As a consequence of the Lee-Yang theorem [24], there can be *no singularities* of the respective partition function at any real nonzero field, ruling out the existence of a quantum phase transition for this model. This implies that the magnetic gap remains finite for any dissipation strength.

An entirely different behavior arises if dissipation is coupled such that it stabilizes the “classical” state of the system. Coupling the bath to either  $\sigma_i^z$  or  $\mu_p^z$  stabilizes the classical state of a single spin or a plaquette, respectively. We consider the latter as it should be more effective at damping quantum fluctuations. Integrating out the heat bath then leads to a model for decoupled Ising chains given by

$$\mathcal{H}_{\text{cl}} = -K_\tau \sum_{k,p} S_k^p S_{k+1}^p - \alpha \sum_{k < k', p} \frac{(\frac{\pi}{N_\tau})^2 S_k^p S_{k'}^p}{\sin^2(\frac{\pi}{N_\tau} |k - k'|)}, \quad (4)$$

where the parameter  $\alpha$  measures the dissipation strength. This model has been studied [25] and is known to exhibit a Thouless-type phase transition into a classically ordered, fluctuationless phase. The critical value  $\alpha_c$  of this transition depends weakly on the cutoff in the long-range interaction; in our simulations  $\alpha_c \approx 0.7$ . At the transition, the magnetic gap vanishes, in sharp contrast to the previous case.

Because of the long-range interactions introduced by the dissipative coupling, the spin-spin correlations asymptotically decay as  $1/\tau^2$  [26] making it nontrivial to define a correlation time. For  $\alpha \lesssim 0.1$  one observes an exponential decay of the correlation function onto the asymptotic  $1/\tau^2$  behavior. The  $\xi_\tau$  extracted from the exponential component grows linearly with  $\alpha$ . For  $\alpha > 0.1$  we estimate  $\xi_\tau$  from the asymptotic decay of the correlations  $\sim (\xi_\tau/\tau)^2$ . These  $\xi_\tau$ s grow approximately exponentially in the region  $0.1 \lesssim \alpha \lesssim \alpha_c$ . Alternatively, one could define a correlation time from the crossover scale where the short-time behavior crosses over to the asymptotic  $1/\tau^2$  form (the results are almost identical). Gap and error probability computed from the inverse correlation length are given in Fig. 6. The error probability remains negligibly small below the crossover value  $\alpha \approx 0.1$ .

*Outlook.*—The topological phase of the toric code exists in an extended region of phase space around the soluble point. This demonstrates that a system does not have to be particularly fine-tuned to reach such a phase. These conclusions need to be tested for other, more exotic topological phases supporting universal quantum computation [27].

We thank E. Ardonne, L. Balents, S. Chakravarty, and A. Kitaev for discussions. C.N. is supported by NSF No. DMR-0411800 and ARO No. W911NF-04-1-0236.

- [1] A. Yu. Kitaev, *Ann. Phys. (N.Y.)* **303**, 2 (2003).
- [2] R. Moessner and S.L. Sondhi, *Phys. Rev. Lett.* **86**, 1881 (2001); C. Nayak and K. Shtengel, *Phys. Rev. B* **64**, 064422 (2001); L. Balents *et al.*, *Phys. Rev. B* **65**, 224412 (2002); M. Freedman *et al.*, *Ann. Phys. (N.Y.)* **310**, 428 (2004); M. A. Levin and X.-G. Wen, *Phys. Rev. B* **71**, 045110 (2005); P. Fendley and E. Fradkin, *Phys. Rev. B* **72**, 024412 (2005).
- [3] L. B. Ioffe *et al.*, *Nature (London)* **415**, 503 (2002).
- [4] O.I. Motrunich and T. Senthil, *Phys. Rev. Lett.* **89**, 277004 (2002).
- [5] L.-M. Duan *et al.*, *Phys. Rev. Lett.* **91**, 090402 (2003); V. Gurarie *et al.*, *Phys. Rev. Lett.* **94**, 230403 (2005).
- [6] A quantum dimer model itself constitutes a quantum loop gas, with the loops appearing in a transition graph with any fixed reference dimer configuration.
- [7] D.S. Rokhsar and S.A. Kivelson, *Phys. Rev. Lett.* **61**, 2376 (1988).
- [8] A. Leggett *et al.*, *Rev. Mod. Phys.* **59**, 1 (1987).
- [9] P. Werner *et al.*, *Phys. Rev. Lett.* **94**, 047201 (2005); P. Werner *et al.*, *J. Phys. Soc. Jpn. Suppl.* **74**, 67 (2005).
- [10] In a special topological phase considered in [11], thermal activation *always* dominates quantum tunneling. The concentration of excitations leading to unrecoverable errors was given in [12].
- [11] C. Chamon, *Phys. Rev. Lett.* **94**, 040402 (2005).
- [12] C. Wang *et al.*, *Ann. Phys. (N.Y.)* **303**, 31 (2003).
- [13] R. Moessner *et al.*, *Phys. Rev. B* **65**, 024504 (2001).
- [14] H. W. J. Blöte and Y. Deng, *Phys. Rev. E* **66**, 066110 (2002).
- [15] In parallel work, model (2) and a similar mapping has been exploited for adiabatic quantum computation [16].
- [16] A. Hamma and D. A. Lidar, *quant-physics/0607145*.
- [17] A.M. Ferrenberg and D. P. Landau, *Phys. Rev. B* **44**, 5081 (1991).
- [18] E. Ardonne *et al.*, *Ann. Phys. (N.Y.)* **310**, 493 (2004).
- [19] F. Alet *et al.*, *J. Phys. Soc. Jpn. Suppl.* **74**, 30 (2005).
- [20] S. Todo and K. Kato, *Phys. Rev. Lett.* **87**, 047203 (2001).
- [21] M. Caselle *et al.*, *J. High Energy Phys.* 01 (2003) 057.
- [22] G. Schön and A. D. Zaikin, *Phys. Rep.* **198**, 237 (1990).
- [23] A. O. Caldeira and A. J. Leggett, *Ann. Phys. (N.Y.)* **149**, 374 (1983).
- [24] T. D. Lee and C. N. Yang, *Phys. Rev.* **87**, 410 (1952).
- [25] D. J. Thouless, *Phys. Rev.* **187**, 732 (1969); J. Fröhlich and T. Spencer, *Commun. Math. Phys.* **84**, 87 (1982); J. Bhattacharjee *et al.*, *Phys. Rev. B* **24**, 3862 (1981); E. Luijten and H. Messingfeld, *Phys. Rev. Lett.* **86**, 5305 (2001).
- [26] R. B. Griffiths, *J. Math. Phys. (N.Y.)* **8**, 478 (1967).
- [27] M. H. Freedman, *Found. Comput. Math.* **1**, 183 (2001).